

Nanoscale Friction: Kinetic Friction of Magnetic Flux Quanta and Charge Density Waves

A. Maeda,^{1,2} Y. Inoue,¹ H. Kitano,¹ Sergey Savel'ev,² S. Okayasu,³ I. Tsukada,⁴ and Franco Nori^{2,5}

¹Department of Basic Science, University of Tokyo, 3-8-1, Komaba, Meguro-ku, Tokyo, 153-8902, Japan

²Frontier Research System, RIKEN, Saitama, 351-0198, Japan

³JAERI, Tokai-mura, Naka-gun, Ibaraki 319-1195, Japan

⁴CRIEPI, 2-11-1, Iwadokita, Komae, Tokyo, 201-8511, Japan

⁵Department of Physics and MCTP, University of Michigan, Ann Arbor, MI 48109-1120, USA

(Received 5 October 2004; published 22 February 2005)

In analogy with the standard macroscopic friction, here we present a comparative study of the friction force felt by moving vortices in superconductors and charge density waves. Using experiments and a model for this data, our observations (1) provide a link between friction at the micro- and macroscopic scales, (2) explain the roundness of the static-kinetic friction transition in terms of thermal fluctuations, particle interactions, and system size (critical-phenomena view), and (3) explain the crossing of the kinetic friction F_k versus velocity V for our pristine (high density of very weak defects) and our irradiated samples (with lower density of deeper pinning defects).

DOI: 10.1103/PhysRevLett.94.077001

PACS numbers: 74.25.Qt, 71.45.Lr, 68.35.Af

Friction forces are very important for a vast range of technological applications. However, the microscopic origin of friction has been a puzzle for over 500 years. Recent advances in atomic force probes are advancing our understanding of the origin of friction at the molecular and atomic scales (see, e.g., [1–4] and references therein). Leonardo da Vinci's velocity-independent friction force, still the standard in many textbooks, is successful at describing friction for many systems, but it fails for others which have a kinetic friction force F_k that changes from its static maximum value F_s .

When a massive block slides on a rough surface through a fluid, the resistive force opposing its motion has two components: one (kinetic friction F_k) from the substrate and an additional (hydrodynamic) viscous force due to the surrounding fluid. Similarly, when tiny magnetic and electric quanta move inside solids, they also experience a resistive force from both the underlying substrate impurities F_k and the surrounding medium. In analogy with the standard macroscopic friction, here we present a comparative study of the friction force felt by moving magnetic flux quanta (vortices) and charge density waves.

Near the threshold for the onset of motion, a driven block accelerates and stops showing “stick-slip” motion, which plays a central role in geology, tribology, and in many industrial processes [3,4]. This stick-slip motion can be viewed as strong fluctuations near the sharp transition [5] between two dynamical states having static F_s and kinetic F_k friction [see also Fig. 1(f)]. Experiments (e.g., [6,7]) support this fluctuation mechanism and pose the question [6] of why in some cases $F_s > F_k$, while in other cases $F_k > F_s$ (for higher temperatures this is equivalent to crossing plots for different $F_k(V)$'s). Our experimental and theoretical results [Fig. 1(c) and 1(d)] also have such crossing points in $F_k(V)$.

Another challenge occurs when trying to bridge micro- and macro-scale descriptions of friction, especially when

trying to measure and characterize friction for very tiny objects, which are not standard “particles,” but collective excitations inside solids, like magnetic flux quanta in superconductors [8] and charge density waves (CDWs) [9]. Here, we present a comparative study of the depinning dynamics of such microscopic objects, described as examples of friction (see Table I and Fig. 1). While some friction experiments are not easy to reproduce, the microscopic friction shown here is perfectly reproducible.

Friction measurements on moving vortices.—Experiments were made on pristine and irradiated $\text{La}_{1.84}\text{Sr}_{0.16}\text{CuO}_4$ (LSCO) superconductors [11] with a critical temperature $T_c = 37$ K over a wide range of magnetic fields and temperatures. As will be shown below, we need V - I characteristics up to high current density. Thus, we used 1800 Å thick single crystalline films prepared by the pulsed laser deposition (PLD) method. The substrate was LaSrAlO_4 (001) with thickness 0.5 mm. To avoid Joule heating, we used short rectangular pulses for the V - I measurements. After removing the flux-flow dissipation (viscous) component [10], the measured friction per unit length (shown in Fig. 1) is $F_k = j\Phi_0(1 - \rho/\rho_\infty)$ where j is the current density, Φ_0 is the flux quantum, and ρ (ρ_∞) is the (flux-flow) resistivity [12,13]. We used microwave techniques to obtain ρ_∞ in bulk crystals with the same hole concentration [12]. In our experiments [Fig. 1(a)] and theory [Fig. 1(b)] the kinetic friction $F_k(V)$ increases with the average velocity V , attaining a maximum, and decreases with magnetic field. Moreover, our measured friction [Fig. 1(c)] for pristine samples is smaller than for irradiated ones at low average velocities V (staticlike regime) and larger for higher V (kineticlike regime). This is consistent with our numerical results [Fig. 1(d)] and also with macroscopic *mechanical* friction experiments performed on solids (e.g., [6]).

Friction in charge density waves.—Measurements on CDWs were performed on single crystals of NbSe_3 ,

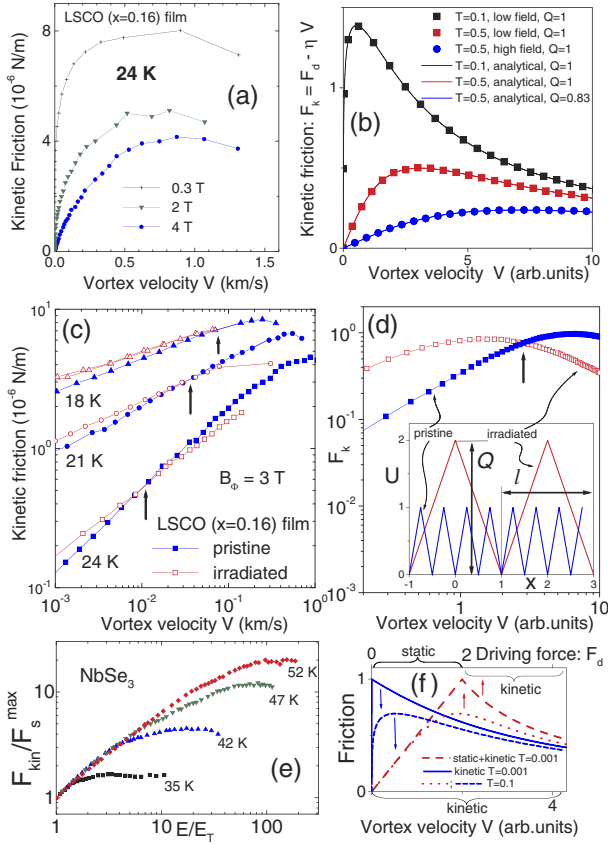


FIG. 1 (color online). Kinetic friction F_k (per unit length of the vortex) versus average velocity V for magnetic vortices in LSCO pristine superconductors (a) and theoretical results in (b). For vortices, $V = H/E =$ magnetic/electric fields. In (a), (b): $F_k(V)$ exhibits a maximum and decreases with vortex density. $T =$ Tesla in (a), (c). For (c), (d): $F_k(V)$ for pristine and 200 MeV-iodine-irradiated (with equivalent field $B_\Phi = \Phi_0/d^2$, d is the average distance between defects) superconductors (c) and theory results in (d). For (c), (d): For low velocities, $F_k(\text{irradiated}) > F_k(\text{pristine})$ (because the irradiation introduces defects that provide large potential barriers, hard to overcome at low velocities, increasing the friction). For high velocities, $F_k(\text{irradiated}) < F_k(\text{pristine})$, because the pristine sample has very many shallow (but steep) pinning sites, effectively providing a large pinning force. A similar broad maximum for $F_k(V)$ [in panels (a)–(d)] was also found for very different excitations: charge density waves (e). All of these properties are well explained [e.g., (b), (d)] with a simple model for overdamped particles discussed in the text. (e) Measured normalized kinetic friction versus driving electric field E (normalized by the threshold field E_T) for the CDW NbSe_3 . Note the similarities between the CDW in (e) and the pristine samples in (c) and (d). (f) Friction versus both: driving force F_d (upper axis) and versus V (lower axis). A sharp (smooth) transition from static to kinetic friction regimes for low (higher) temperatures is clearly seen. Note that $F_k(V \rightarrow 0) = F_s \neq 0$.

grown by the direct vapor transport (DVT) method. Here, E (E_T) is the (threshold) electric field and σ_{CDW} (σ_∞) is the extra conductivity of the CDW (in the high-field limit), which was obtained by the pulse technique.

Figure 1(e) shows $F_{\text{kin}}/F_{\text{max}} = [1 - \sigma_{\text{CDW}}(E)/\sigma_\infty]E/E_T$. The first term in the right-hand side is the driving force by the electric field E and the second term subtracts the average viscous dissipation [14,15], corresponding to the flux-flow dissipation for vortices [13] and the hydrodynamic resistance due to the surrounding fluid in the mechanical case. The result is normalized by the depinning field E_T , corresponding to the critical current density j_c in the superconducting case and the maximum static-friction force F_s^{max} for a massive block.

The conductivity $\sigma_{\text{CDW}}(E)$ is measured by current-voltage (I - V) plots, while the resistivity ρ for vortices in superconductors is obtained from V - I measurements [13]. Thus, our F_{kin} measurements on CDWs have direct analogs with the corresponding F_{kin} for vortices or sliding massive blocks. Note that CDW scattering with phason or quasiparticles and fixed impurities are the analogs of the vortex dissipative flux flow and pinning, respectively.

Numerical results.—Since experiments were performed at high enough temperatures, thermal fluctuations are dominant over quantum fluctuations. The simplest minimal model to describe all of these properties is the overdamped equation (commonly used for vortices and CDWs):

$$\eta v_i = -\frac{\partial}{\partial x_i} \left[U(x_i) + \sum_j W(x_i - x_j) \right] + F_d + \xi(t), \quad (1)$$

where x_i and v_i are the positions and velocities (of vortices or CDWs), $U(x)$ is the (substrate) pinning potential [inset of Fig. 1(d)], F_d is the driving force, T is the temperature, η is the effective viscosity, W describes the intervortex interactions, and ξ is the thermal random force with zero average $\langle \xi \rangle = 0$ and autocorrelations $\langle \xi(0)\xi(t) \rangle = 2k_B T \delta(t)$. The transition to the macroscopic case can be seen by considering a macroscopic block containing $N \gg 1$ strongly-coupled particles. Associating a collective coordinate $x_{\text{block}} = \sum x_i/N$ to this block and averaging out Eq. (1), we derive another Langevin equation with a new stochastic variable $\zeta = \sum \xi/N$, $\langle \zeta(0)\zeta(t) \rangle = \delta(t)$ and effective temperature $T^{\text{eff}} = T/N$. Thus, thermal effects decrease with system size L as $T^{\text{eff}} \propto T/L^3$ and become negligible for macroscopic blocks.

Results from this model are shown in Figs. 1(b) and 1(d) in qualitative agreement with our data in Figs. 1(a), 1(c), and 1(e). At low temperatures, and when driving close to its critical value, we also obtain long random waiting times, when a particle remains trapped in a potential well and sometimes does fast jumps between wells. This corresponds to the stick-slip motion for macroscopic blocks. At higher temperatures, and larger particle densities, this transition from static to kinetic friction becomes smooth.

Analytical results.—Neglecting interparticle interactions, the Langevin Eq. (1) can be mapped onto a Fokker-Planck equation, which can be solved analytically for a time-independent driving force F_d :

TABLE I. Comparison between mechanical friction and friction for vortices in superconductors (SC) and charge density waves (CDW). If a driven block slides on a rough surface, the resistive force on the block has two components: one due to the interaction with the substrate (standard kinetic friction F_k) and an additional (hydrodynamic) resistance if the driven block is submerged in a fluid (e.g., molasses). Similarly to a massive sliding block driven in molasses, when a vortex moves inside a superconductor, it experiences a resistive force because of the surrounding superfluid interacting with the vortex core. This dissipative flux flow exists even when the sample has zero pinning impurities. Therefore, this component must be subtracted [10] from the measured resistive force: to obtain the kinetic friction F_k due to the interaction between the vortex and the pinning “substrate.” Thus, pinning adds additional friction (denoted here by F_k) to moving vortices. Here, $P_{\text{dissipated}}$ is the power dissipated during motion and ω is the driving frequency.

System	Mechanical Friction	Vortices in Superconductors	Charge Density Waves
Movable objects	Blocks, films, etc.	Vortices (magnetic quanta)	Electrons (electric quanta)
Driving force F_d	Mechanical force F_d	Lorentz force $\propto j$	Electric force $\propto E$
Static friction F_s due to	Surface roughness, molecular forces, etc.	Defects, impurities, disorder	Impurities, commensurability of CDW with ions
Critical parameter ($\max F_s$)	Maximum static friction F_s^{\max}	Critical current density j_c	Depinning electric field E_T
Dynamical events	Stick-slip motion	Flux bundle motion	Current (sliding CDW)
Static resistance	Static friction F_s	Pinning (F_{pinning})	Pinning (F_{pinning})
Dynamic resistance due to substrate	Kinetic friction F_k	Kinetic friction F_k (slow down due to pinning)	Interaction with impurities
Hydrodynamic resistance (due to surrounding “fluid”)	Viscosity η , ($P_{\text{dissipated}} = \eta V^2$)	Dissipative flux flow $\propto \rho$, ($P_{\text{dissipated}} = \rho j^2$)	Dissipative sliding CDW; viscosity $\propto \sigma_{\text{CDW}}$, ($P_{\text{dissipated}} = \sigma_{\text{CDW}} E^2$)
Inertial term	Important	Negligible	Important at high ω
Transition from F_s to F_k	Very sharp	Broadens with T and H	Broadens with T
Thermal fluctuations	Not important	Important	Important

$$V(F_d, T, Q, l) = \frac{l(F_d^2 - 4Q^2/l^2)}{\eta[F_d l + k_B T \alpha(T)]}, \quad F_k(F_d, T, Q, l) = F_d - \eta V = \frac{k_B T F_d \alpha(T) + 4Q^2/l}{F_d l + k_B T \alpha(T)}, \quad (2)$$

$$\alpha(T) = \frac{16Q^2[\cosh(F_d l/2k_B T) - \cosh(Q/k_B T)]}{(4Q^2 - F_d^2 l^2) \sinh(F_d l/2k_B T)},$$

where Q and l are the energy barrier height and the typical length scale of the substrate potential, respectively; $\alpha(T)$ is the prefactor of the thermal energy. In Eqs. (2), the ratio $Q/k_B T$ represents the competing pinning/depinning effects of the pin energy barrier Q over the thermal energy, while $F_d l/k_B T$ represents the effects of the driving and thermal energies. According to Eqs. (2), at zero temperature, F_k is a monotonically decreasing function of F_d (as it is usually the case for friction in mechanical blocks, where temperature effects are negligible). For finite temperature, F_k has a maximum for nonzero F_d or V .

The effects of particle interactions can be effectively taken into account by the flattening of the substrate potential due to the mutual repulsion of the moving particles [16]. This results in the decrease of $Q(n)$ with particle density n . From our analytical results, we can derive a broad transition from static to kinetic friction as a function of both temperature *and/or* applied magnetic field $H = \Phi_0 n$ for vortices—because the activation $Q(n)/T$ is suppressed by increasing either T or H . Note that some interaction-related effects, including elastic and plastic deformations of the sliding phase, could be missed in this

simple approach. While plastic dynamics can play a role in some regimes of vortex physics (e.g., near the onset of depinning), it is not a dominant effect in CDWs, where the shear modulus is large. In spite of its limitations, our analytical results describe both our experiments and our numerical simulations of the Langevin Eq. (1) [see Fig. 1(b) for a quantitative comparison of simulations with analytical results]. Moreover, in the limit $Q \ll k_B T$, the function $F_k(F_d)$ increases linearly at low driving forces F_d with a temperature-independent slope, as experimentally observed in Fig. 1(e).

Additional discussions.—For microscopic objects, but not for macroscopic ones, thermal fluctuations play a crucial role broadening the transition between static and kinetic friction [Fig. 1(f)]. The broad transition (Fig. 1) from static to kinetic friction not only can be described by the above model but can also be understood from the perspective of phase transitions [2,5]: sharp transitions for large objects become much broader for small systems.

For our data [Figs. 1(a), 1(c), and 1(e)] and for our simulations and analytical results [Figs. 1(b), 1(d), and 1(f)], the friction force attains its maximum and decreases

with vortex density because the surface “roughness” or pinning becomes less influential in that limit.

Moreover, the deepening and widening pinning potentials [inset of Fig. 1(d)] for modeling irradiated samples qualitatively reproduce all experimental findings [see Figs. 1(c) and 1(d), including the crossing of different $F_k(V)$'s]. The crossing $F_k(V)$'s [e.g., arrows in Figs. 1(c) and 1(d)] are due to the competition between thermal-activated ($\propto \exp(-U/T)$) jumping of barriers (at low velocities) [17] and strongly-driven motion above the depinning force. Indeed, for weak driving (i.e., for thermal-activated jumps) the friction F_k is larger when barriers Q are larger, while for stronger driving F_k increases with Q/l , which results in the crossing of the $F_k(V)$'s curves. Using the collective pinning approach [18], we estimate $Q \propto H_{c1}^{2/3} H_c^{4/3} \xi^2$ and $l \approx \xi$ for pristine samples and $Q \propto H_c^2 \xi^2$ and $l = r_p > \xi$ for irradiated samples, where H_{c1} and H_c are the first critical and thermodynamic fields, and ξ and r_p are the coherence length and the effective radius of the columnar defects. Thus, the crossing point of the $F_k(V)$'s curves can be expected for $r_p \geq \xi(H_c/H_{c1})^{2/3} \sim 5\xi \sim 100 \text{ \AA}$, which are consistent with the estimate $r_p \geq 130 \text{ \AA}$ for our irradiated samples. In addition, thermal and interparticle-repulsion effects both smooth out the crossover between the static (or “almost-static thermal-activated”) and the (strong-driving) kinetic regimes. This broad crossover replaces the sharp transition observed in macroscopic mechanical stick-slip motion.

Measurements of friction [Fig. 1(e)] for electrical microscopic “quasiparticles,” CDWs, also show a smooth increase of the friction with driving force and other features in $F_k(V)$ which are similar to vortex friction, including the broad transition due to the crucial contribution of thermal fluctuations to nanoscale friction (absent in macroscopic descriptions) since $F_k(V)$ smoothly grows with V and T in Fig. 1(e) (in contrast to the typical sharp transition from static to kinetic friction for macroscopic objects).

The CDW-SC comparison can be made more closely. When the CDW and vortex lattices (VLs) are driven, their dynamical response is shaped by the competition between elastic properties (keeping the CDW and VL together) and pinning strength (providing friction that can either stop the CDW-VL or sometimes tear apart the CDW-VL). In equilibrium, the competition between the elastic and pinning energies (for CDWs and VLs) has been studied by using essentially the same model: see, e.g., the Fukuyama-Lee-Rice model in Refs. [19–21] for CDWs and the Larkin-Ovchinnikov model in Ref. [22] for VLs. In both cases, when the elastic energy is large, increased pinning leads to a localization of the CDW-VL (static-friction regime) with large correlated domains in the CDW-VL. When the elastic energy becomes weaker, eventually, the CDW-VL breaks apart into smaller uncorrelated domains which exhibit a plastic response when driven. For very strong drives, compared to the pinning energies, the CDW-VL behaves like an elastic medium and it exhibits dynamic friction. This

highlights another profound analogy in the way pinning and elastic energies behave in these two apparently dissimilar systems which are dual to each other [23].

Here we have compared the kinetic friction related to the collective motion of quanta of magnetic flux and electrical charge, using an approach similar to the one typically used for moving massive blocks (Fig. 1 and Table I). Our results provide a link between friction at the micro- and macroscopic scales.

We acknowledge partial support from the NSA and ARDA, under AFOSR Contract No. 620-02-1-0334, and also by the US NSF Gant No. EIA-0130383.

-
- [1] J. Gao *et al.*, *J. Phys. Chem.* **108**, 3410 (2004).
 - [2] *Springer Handbook of Nanotechnology*, edited by B. Bhushan (Springer, Berlin, 2004).
 - [3] E. Rabinowicz, *Friction and Wear of Materials* (Wiley, New York, 1995), Chap. 4, 2nd ed.
 - [4] F. P. Bowden and D. Tabor, *The Friction and Lubrication of Solids* (Clarendon Press, Oxford, 1986).
 - [5] P. A. Thompson and M. O. Robbins, *Science* **250**, 792 (1990).
 - [6] G. Reiter, A. L. Demirel, and S. Granick, *Science* **263**, 1741 (1994).
 - [7] A. L. Demirel and S. Granick, *Phys. Rev. Lett.* **77**, 4330 (1996).
 - [8] E. H. Brandt, *Rep. Prog. Phys.* **58**, 1465 (1995).
 - [9] L. P. Gor'kov and G. Grüner, *Charge Density Waves in Solids* (North-Holland, Amsterdam, 1990).
 - [10] H. Matsukawa and H. Fukuyama, *Phys. Rev. B* **49**, 17286 (1994).
 - [11] I. Tsukada, *Phys. Rev. B* **70**, 174520 (2004).
 - [12] Y. Tsuchiya *et al.*, *Phys. Rev. B* **63**, 184517 (2001).
 - [13] M. Kunchur *et al.*, *Phys. Rev. Lett.* **84**, 5204 (2000); **89**, 137005 (2002).
 - [14] A. Maeda *et al.*, *J. Phys. Soc. Jpn.* **59**, 234 (1990).
 - [15] P. Littlewood, *Phys. Rev. B* **36**, 3108 (1987); S. N. Coppersmith and P. B. Littlewood, *Phys. Rev. B* **31**, 4049 (1985).
 - [16] S. Savel'ev, F. Marchesoni, and F. Nori, *Phys. Rev. Lett.*, **91**, 010601 (2003); **92**, 160602 (2004).
 - [17] A. Krämer and M. L. Kulić, *Phys. Rev. B* **48**, 9673 (1993).
 - [18] G. Blatter *et al.*, *Rev. Mod. Phys.* **66**, 1125 (1994).
 - [19] H. Fukuyama and P. A. Lee, *Phys. Rev. B* **17**, 535 (1978).
 - [20] P. A. Lee and T. M. Rice, *Phys. Rev. B* **19**, 3970 (1979).
 - [21] L. Sneddon, M. C. Cross, and D. S. Fisher, *Phys. Rev. Lett.* **49**, 292 (1982).
 - [22] A. I. Larkin and Y. N. Ovchinnikov, *J. Low Temp. Phys.* **34**, 409 (1979).
 - [23] Note that these two examples (magnetic and electric collective transport) are dual to each other. Thus, the equations for kinetic friction for moving vortices or CDWs are the same after replacing the current density j by the electric field E and the resistivity ρ by the conductivity. The mapping becomes: [driving force $\leftrightarrow j \leftrightarrow E$], and [viscous dissipation $\leftrightarrow \rho \leftrightarrow \sigma$] for [mechanical \leftrightarrow magnetic \leftrightarrow electric] driven transport. Therefore, V - I curves for superconductors map into I - V curves for CDW transport.